Instantaneous Band Gap Collapse in Photoexcited Monoclinic VO_2 due to Photocarrier Doping

Daniel Wegkamp,[1] Marc Herzog,[1] Lede Xian,[2,3] Matteo Gatti,[4,3,5] Pierluigi Cudazzo,[2,3] Christina L. McGahan,[6] Robert E. Marvel,[6] Richard F. Haglund, Jr.,[6] Angel Rubio,[2,7,3,1] Martin Wolf,[1] and Julia Stähler[1,*]

[1]*Fritz-Haber-Institut der Max-Planck-Gesellschaft, Abteilung Physikalische Chemie, Faradayweg 4-6, 14195 Berlin, Germany*
[2]*Nano-Bio Spectroscopy group, Universidad del País Vasco CFM CSIC-UPV/EHU-MPC & DIPC, 20018 San Sebastián, Spain*
[3]*European Theoretical Spectroscopy Facility (ETSF)*
[4]*Laboratoire des Solides Irradiés, École Polytechnique, CNRS-CEA/DSM, F-91128 Palaiseau, France*
[5]*Synchrotron SOLEIL, L'Orme des Merisiers, Saint-Aubin, BP 48, F-91192 Gif-sur-Yvette, France*
[6]*Department of Physics and Astronomy and Interdisciplinary Materials Science Program, Vanderbilt University, Nashville, Tennessee 37235-1807, USA*
[7]*Max Planck Institute for the Structure and Dynamics of Matter, Luruper Chaussee 149, 22761 Hamburg, Germany*

(Received 15 July 2014; published 17 November 2014)

Using femtosecond time-resolved photoelectron spectroscopy we demonstrate that photoexcitation transforms monoclinic VO_2 quasi-instantaneously into a metal. Thereby, we exclude an 80 fs structural bottleneck for the photoinduced electronic phase transition of VO_2. First-principles many-body perturbation theory calculations reveal a high sensitivity of the VO_2 band gap to variations of the dynamically screened Coulomb interaction, supporting a fully electronically driven isostructural insulator-to-metal transition. We thus conclude that the ultrafast band structure renormalization is caused by photoexcitation of carriers from localized V 3*d* valence states, strongly changing the screening before significant hot-carrier relaxation or ionic motion has occurred.

DOI: 10.1103/PhysRevLett.113.216401 PACS numbers: 71.27.+a, 71.20.Be, 71.30.+h, 79.60.-i

Since its discovery in 1959 [1], studies of the VO_2 phase transition (PT) from a monoclinic (M_1) insulator (Fig. 1, top left) to a rutile (R) metal at $T_C = 340$ K (Fig. 1, top right) have revolved around the central question [2–5] of whether the crystallographic PT is the major cause for the electronic PT or if strong electron correlations are needed to explain the insulating low-T phase. While the M_1 structure is a necessary condition for the insulating state below T_C, the existence of a monoclinic metal (mM) and its relevance to the thermally driven PT is under current investigation [6–12]. In particular, the role of carrier doping at temperatures close to T_C by charge injection from the substrate or photoexcitation has been increasingly addressed [6,8,13–16].

One promising approach to disentangling the electronic and lattice contributions is to drive the PT nonthermally using ultrashort laser pulses in a pump-probe scheme. Time-resolved x-ray [17,18] and electron diffraction [16,19] showed that the lattice structure reaches the R phase quasithermally after picoseconds to nanoseconds. Transient optical spectroscopies have probed photoinduced changes of the dielectric function in the terahertz [20–22], near-IR [9,10,17,23], and visible range [23]. The nonequilibrium state reached by photoexcitation (hereinafter transient phase) differs from the two equilibrium phases, but eventually evolves to the R phase [17–28]. The observation of a minimum rise time of 80 fs in the optical response after strong excitation (50 mJ/cm^2), described as a *structural bottleneck* in VO_2 [24], challenged theory to describe the photoinduced crystallographic and electronic PT simultaneously [15,25].

Time-resolved photoelectron spectroscopy (TR-PES) directly probes changes of the electronic structure. Previous photoelectron spectroscopy (PES) studies of VO_2 used high photon energies generating photoelectrons with large kinetic energies to study the dynamics of the electronic structure; however, with a low repetition rate (50 Hz [27]) and inadequate time resolution (> 150 fs) the ultrafast dynamics of the electronic PT were inaccessible [28]. Thus, fundamental questions—namely, how fast and why the band gap closes and whether this happens before or simultaneously with the crystallographic PT (Fig. 1, top, center)—remained unanswered.

In this Letter, we use TR-PES to directly monitor the photoinduced changes of the density of states (DOS) around the Fermi energy E_F, which define the conduction properties of VO_2. We show that the insulating gap collapses during the exciting laser pulse (< 60 fs) with no sign of a structural bottleneck. The transient phase is an excited mM with carrier relaxation times on the order of 200 fs. This interpretation of the experimental results is supported by first-principles calculations based on many-body perturbation theory. They reveal that the band gap in the M_1 phase is extremely sensitive to small changes in the occupation of the localized d bands that alter the dynamically screened Coulomb interaction. We thereby identify the origin of the metallization: photoexcitation induces

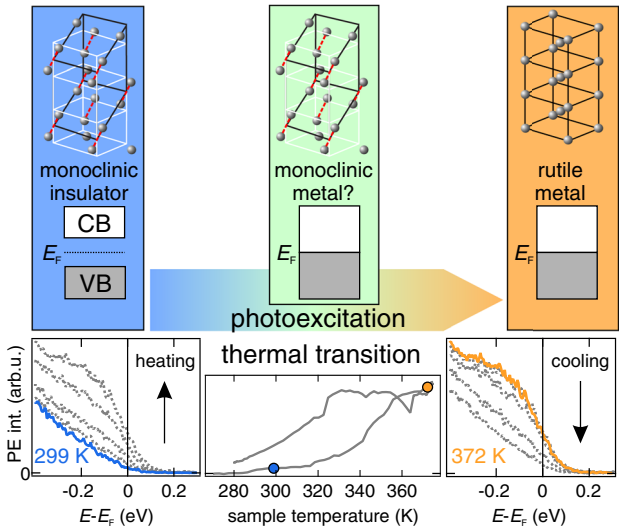

FIG. 1 (color online). Top: the photoinduced PT from the insulating M_1 phase (left) to the metallic R phase (right) could proceed via a transient mM phase (green) or concurrently with the structural PT. Gray balls illustrate the V atom positions. Bottom: heating leads to the buildup of the photoemission (PE) intensity in the band gap (left), which is depleted upon cooling (right). Integrated PE intensity (-0.2 eV $< E - E_F <$ 0.0 eV) exhibits a hysteresis (center).

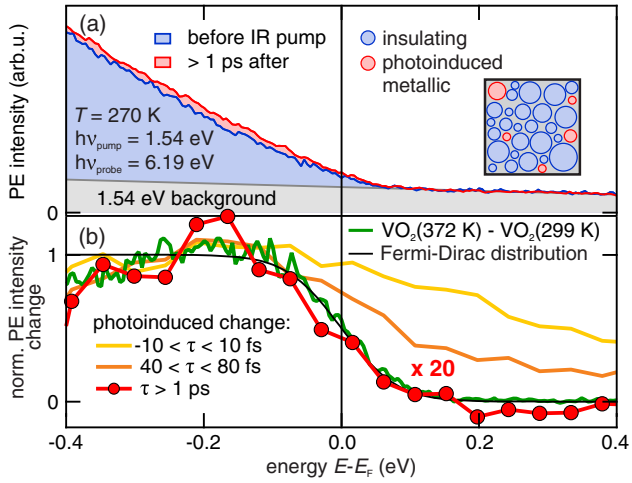

FIG. 2 (color online). (a) Photoelectron spectra before (blue) and > 1 ps after pump (red, 6.7(8) mJ/cm^2). Inset: illustration of partial switching of selected domains. (b) Comparison of thermally induced (green) and persistent photoinduced change (yellow, orange, red). The latter spectra were binned in energy at a step size of $\Delta E = 45$ meV.

holes by depletion of the V 3d valence orbital population [29,30], strongly affecting the screening and collapsing the band gap. Finally, the analysis demonstrates that, due to their strong localization, photoinduced holes are more effective than electrons in driving band gap renormalization. In fact, hole doping can completely close the gap without the need of a structural change, thus initiating a "hole-driven insulator-to-metal transition."

The 45 nm epitaxial VO_2 film on a c-cut sapphire crystal was grown at room temperature by pulsed laser ablation of a V target in oxygen [31]. For PES, it is kept under ultrahigh vacuum conditions and prepared by annealing cycles in an oxygen atmosphere. TR-PES is performed using a regeneratively amplified femtosecond laser working at a repetition rate of 40 kHz. A pump pulse ($h\nu_{pump} = 1.54$ eV) launches the nonequilibrium dynamics and its fourth harmonic ($h\nu_{probe} = 6.19$ eV) serves as probe pulse for photoemission. The incident pump fluence was 6.7(8) mJ/cm^2 (approximately 0.08 electrons per V atom) and the probe fluence was kept below 8 μJ/cm^2 to avoid charging of insulating VO_2 and space-charge effects [32].

Figure 1 bottom (left and right) depicts the photoelectron spectra of VO_2 in equilibrium at energies within the ≈0.6 eV band gap of the insulating phase [33]. The blue curve (299 K) exhibits the high-energy tail of the VO_2 valence band (VB). Heating the sample leads to a buildup of intensity (dotted curves, left) and a Fermi-Dirac (FD)-like spectrum centered around E_F at 372 K (orange curve). This thermally induced photoemission (PE) intensity is suppressed upon cooling (dotted curves, right). The spectral weight below E_F follows a hysteresis centered at 330 K with a width of 25 K (center panel) in line with optical experiments [32]. The difference between the high- and low-temperature photoelectron spectra is plotted in Fig. 2(b) (green). Because of the excellent agreement of the thermally induced change of the PE intensity with the parameter-free FD distribution for 372 K (black) [34], we conclude that, using $h\nu_{probe} = 6.19$ eV, we are sensitive to the electronic PT in VO_2.

In order to elucidate how the photoinduced electronic PT evolves, we perform *time-resolved* PES. We expect photoinduced changes on the order of 1%–10% of the thermally induced change, as reported for optical experiments at comparable pump fluences [10,17,26]. This is because only parts of the probed volume are transformed into the transient phase [Fig. 2(a), inset] at excitation densities below the saturation regime ($F_{sat} \approx 4F_{TH}$, where F_{TH} is the threshold fluence for the PT) [16,24,26] similar to the thermally driven PT [12,35]. While optical experiments probe photoinduced changes due to carrier dynamics in the conduction band (CB) and VB of insulating VO_2 and close to E_F of (potentially photoexcited) metallic VO_2, the energy selectivity of PES permits us to exclusively monitor photoinduced changes due to metallization by probing the dynamics in the gap of insulating VO_2. Figure 2(a) shows the photoelectron spectra before (blue) and > 1 ps after the pump pulse. Indeed, the photoinduced change is very small. The difference is plotted in Fig. 2(b) (red markers) and compared to the thermally induced metallic spectral function (green).

As in optical experiments at comparable excitation fluences (see, e.g., Ref. [26]), the photoinduced signal is considerably smaller than the thermally induced one (here 5%). Yet, the curves show remarkable agreement, implying

that the pump pulse has metallized individual grains of the sample [Fig. 2(a), inset]. Moreover, the signature of this transient metallic phase is practically identical with that of the thermally switched rutile VO_2. This direct observation of metallicity (defined by the presence of a Fermi edge) in photoexcited VO_2 on ultrafast time scales goes beyond optical probes of metal-like dielectric functions, because those can be influenced strongly by a highly excited electron-hole plasma in the CB and VB or structural changes that alter the dielectric function [36].

Figure 3 presents the ultrafast dynamics of the photoinduced electronic PT. The pump-induced change of the PE intensity is depicted in false colors [Fig. 3(a)] and is characterized by a fast component (femtosecond time scales) and a long-lived intensity below E_F, which is spectrally equivalent to the photoinduced change in Fig. 2(b). More precisely, the pump-induced intensity below E_F represents the spectral signature of the transient metallic phase. Fully established at 1 ps, it is never modulated by coherent oscillations and remains unchanged for up to 400 ps (not shown). This is noteworthy, as some time-resolved diffraction experiments on VO_2 demonstrate an evolution of the atomic lattice over nanoseconds [16–19]. The invariance of the time-resolved photoelectron spectra on picosecond time scales shows that intermediate steps of the crystallographic PT have no effect on the FD distribution observed here, implying that the photoinduced electronic PT, i.e., the band gap collapse, is completed before 1 ps elapses.

Note that the photoinduced *change* of the time-resolved PE signal in the gap below E_F results only from individual pump-induced metallized crystal domains, as photoexcited carrier dynamics in insulating VO_2 would occur at different energies (in the CB and VB). Thus, the PE intensity above E_F [purple bar in Fig. 3(a)] corresponds to excited electrons in the transient (metallic) phase and the PE intensity below E_F (green bar) to dynamics in its occupied electronic band structure. The latter cannot result from defect states in the gap, as these would already be occupied in equilibrium [37]. The temporal evolution of the integrated PE intensity in these energy windows is shown in Fig. 3(b). Both traces are well fit by single exponential decays (black curves) with constant offsets [38], convolved with the laser pulse envelope (duration: 61(5) fs [32]). The fits yield average decay constants $\tau_e = 160(70)$ fs and $\tau_h = 210(60)$ fs. Importantly, the PE intensity in the gap is observed quasi-instantaneously at photoexcitation. We do not observe a delayed rise of intensity below E_F with a time scale of 80 fs as expected for a structural bottleneck [24,32]. On the contrary, the photoinduced PE intensity decreases on a time scale of 210 fs as expected for hole relaxation towards E_F from lower energies. Figure 2(b) depicts difference photoelectron spectra at $t = 0$ and 60 fs. They clearly display transiently occupied states close to E_F, superimposed by the lifetimeless intensity from two-photon absorption through virtual states. Therefore, the electronic PT occurs with the

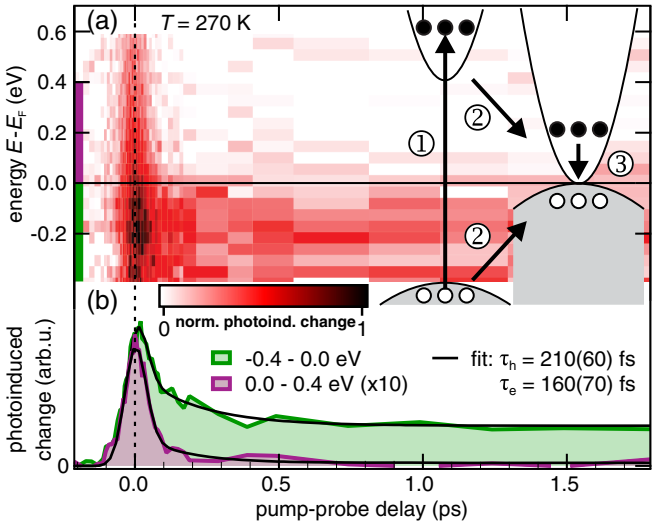

FIG. 3 (color online). (a) PE intensity change versus pump-probe delay close to E_F. Photoelectrons are detected immediately in the gap, showing the quasi-instantaneous collapse (cf. cartoon, energy axis is to scale). Integration of the PE intensity above (purple) and below (green) E_F yields the respective transients in (b). The empirical fit (black) quantifies the averaged hot electron (hole) lifetimes [32].

photoexcitation of the electronic structure and precedes any significant ionic motion towards the R phase.

In order to identify the physical mechanism for ultrafast metallization of photoexcited VO_2, we performed first-principles calculations of the quasiparticle DOS within a many-body Green's function approach [32,39]. We adopted the GW approximation for the self-energy Σ [40], because the quasiparticle self-consistent GW approximation, which naturally accounts for the localized character of the V $3d$ electrons, yields reliable quasiparticle band structures [41,42] compared to experiments [33]. Alternatively, cluster DMFT (dynamical mean-field theory) is also able to describe the electronic structure of monoclinic VO_2 [5,43]. In the GW approximation Σ is given by the product of the one-particle Green's function G and the dynamically screened Coulomb interaction $W(\omega) = \varepsilon^{-1}(\omega)v$. Here v is the bare Coulomb interaction and ε^{-1} is the inverse dielectric function calculated in the random-phase approximation including electron-hole and plasmon excitations [32].

The abruptness of the experimentally observed gap collapse justifies a Born-Oppenheimer approach with a "frozen lattice." In this spirit, we redistribute a portion of the VB electrons equivalent to the experimental excitation density (0.075 electrons per V atom) to the unoccupied states. Note that our findings are robust with respect to excitation density [32]. We then calculate the screened interaction ΔW that is changed by the presence of the additional carriers and the quasiparticle DOS with the self-energy $\Delta\Sigma = G\Delta W$ [32,44]. This redistribution of the electron and hole populations in the VB and CB is sufficient to lead to a collapse of the band gap [Fig. 4(a)].

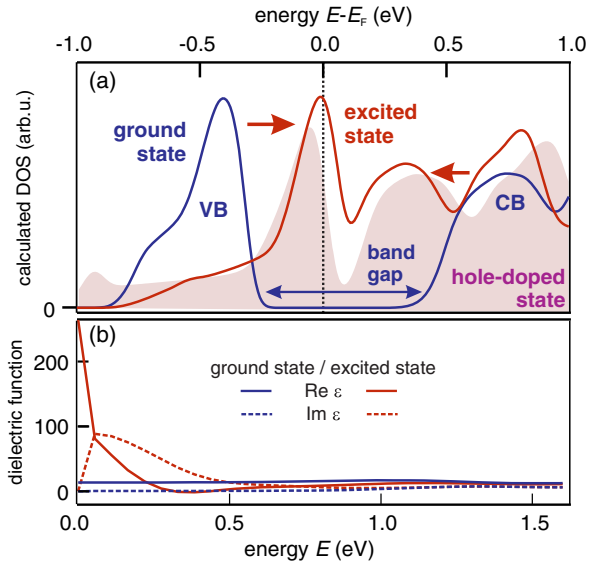

FIG. 4 (color online). (a) Calculated DOS (integrated over the entire Brillouin zone) of the M_1 ground (blue) and excited states (red) broadened by the experimental resolution (90 meV). (b) Real and imaginary parts of the dielectric function $\varepsilon(\omega)$ for a representative small momentum transfer $\mathbf{q} = (1/6, 0, 0)$.

In contrast to ordinary semiconductors where free-carrier doping leads to a moderate band gap narrowing [44–48] and never results in a complete band gap collapse purely electronically [48], this extreme sensitivity of VO_2 to changes of the V $3d$ occupation is a distinctive and unique property of correlated materials [49].

The dynamical screening in fact increases significantly in the low-energy region [<1.5 eV, see $\mathrm{Re}\,\varepsilon(\omega)$ and $\mathrm{Im}\,\varepsilon(\omega)$ in Fig. 4(b)] due to creation of new VB-VB and CB-CB intraband electron-hole channels in the photoexcited system, while it remains almost unchanged in the high-energy region. This finding is robust with respect to variations of the charge redistributions involving the depopulation of the V $3d$ bands [32]. In order to unravel the microscopic mechanism at the origin of the band gap collapse, we separately analyze the effect of changing the occupations of only the VB or CB. We find that hole doping at the top of the VB alone indeed induces the band gap breakdown [32] as suggested before [50]. We rationalize these findings by the fact that VO_2 possesses an almost nondispersive top VB corresponding to localized V $3d$ states [41,51]. Population changes of these states strongly enhance low-energy screening, leading to instantaneous metallization (band gap closure). Note that pure electron doping also leads to a reduction of the band gap but without metallization (no band gap closure) [32].

The relevant elementary processes are sketched in the inset of Fig. 3(a). Absorption of pump photons lifts localized electrons from the top VB into the CB of insulating VO_2. This photocarrier doping causes an instantaneous breakdown of the gap [52] and excited electrons and holes subsequently relax at a slower rate towards equilibrium at E_F. The experimentally determined hot carrier relaxation times of order 200 fs agree nicely with observations from other experiments. A similar time constant characterizes the incoherent time-dependent response of the conductivity in the terahertz measurements of Pashkin *et al.* [22], which may well originate from excited carriers in the CB of VO_2. Also, pump-probe experiments of the transient phase revealed that the optical response of photoexcited VO_2 starts to resemble that of the thermally metallized sample after 200 fs [26]. Photoexcitation of VO_2 creates an excited metal whose optical and electronic properties become similar to those of the thermally driven material only after the hot carriers have equilibrated. It is possible that the subsequent evolution of photoexcited VO_2 towards the R phase occurs quasithermally, as the hot carriers thermalize with the lattice and heat it above T_C. Unlike the thermal PT, where lattice distortion and Coulomb interaction cooperatively drive the formation of the insulating gap, photoexcitation of the *electronic* system instantaneously modifies the *electronic correlations* causing the gap collapse, which is subsequently stabilized by the structural evolution.

In conclusion, the present experimental and theoretical work provides a comprehensive description of the elementary steps of the photoinduced electronic PT in VO_2. The band gap of the insulating phase collapses instantaneously upon photoexcitation due to carrier doping, revealing an ultrasensitivity of VO_2 to variations of the screening by holes at the top of the V valence bands. The band gap collapse is followed by hot carrier relaxation in the transient metallic phase on a 200 fs time scale and quasithermal evolution of the system towards the high-T phase. The abrupt vanishing of the band gap proves the absence of a structural bottleneck in the photoinduced electronic PT [36]. Moreover, the electronic PT precedes the time scales observed for the crystallographic PT [18,19], in excellent agreement with recent observations of a photoexcited mM-like VO_2 [16]. These new insights into the character of the isostructural insulator-to-metal transition in VO_2 provide not only a novel understanding of the physical mechanisms of the phenomenon, but also establish the basis for new experimental and theoretical studies of photoinduced dynamics in the transient metallic phase of VO_2 as well as other correlated materials.

We gratefully acknowledge intense and fruitful discussions with S. Wall and A. Leitenstorfer and very useful comments from L. Perfetti about sample preparation. R. E. M., C. L. M., and R. F. H. were supported by the National Science Foundation (Grant No. DMR-1207507). A. R., P. C., and L. X. acknowledge support by the European Research Council Advanced Grant DYNamo (Grant No. ERC-2010-AdG-267374) and Grupos Consolidados UPV/EHU del Gobierno Vasco (IT-578-13). A. R., P. C., L. X., M. W., and J. S. received support from the European Commission project CRONOS (Grant No. 280879-2) and M. G. from a Marie Curie FP7 Integration Grant within the 7th European Union Framework Programme. Computational time

was granted by Grand Equipement National de Calcul Intensif (Project No. 544) and Barcelona Supercomputing Center "Red Espanola de Supercomputacion." D. W. acknowledges support from the Leibniz Graduate School DinL.

*staehler@fhi-berlin.mpg.de

[1] F. J. Morin, Phys. Rev. Lett. **3**, 34 (1959).
[2] J. B. Goodenough, J. Solid State Chem. **3**, 490 (1971).
[3] A. Zylbersztejn and N. F. Mott, Phys. Rev. B **11**, 4383 (1975).
[4] R. M. Wentzcovitch, W. W. Schulz, and P. B. Allen, Phys. Rev. Lett. **72**, 3389 (1994).
[5] S. Biermann, A. Poteryaev, A. I. Lichtenstein, and A. Georges, Phys. Rev. Lett. **94**, 026404 (2005).
[6] H.-T. Kim, Y. W. Lee, B.-J. Kim, B.-G. Chae, S. J. Yun, K.-Y. Kang, K.-J. Han, K.-J. Yee, and Y.-S. Lim, Phys. Rev. Lett. **97**, 266401 (2006).
[7] E. Arcangeletti, L. Baldassarre, D. Di Castro, S. Lupi, L. Malavasi, C. Marini, A. Perucchi, and P. Postorino, Phys. Rev. Lett. **98**, 196406 (2007).
[8] Z. Tao, T.-R. T. Han, S. D. Mahanti, P. M. Duxbury, F. Yuan, C.-Y. Ruan, K. Wang, and J. Wu, Phys. Rev. Lett. **109**, 166406 (2012).
[9] T. L. Cocker, L. V. Titova, S. Fourmaux, G. Holloway, H.-C. Bandulet, D. Brassard, J.-C. Kieffer, M. A. El Khakani, and F. A. Hegmann, Phys. Rev. B **85**, 155120 (2012).
[10] W. P. Hsieh, M. Trigo, D. A. Reis, G. A. Artioli, L. Malavasi, and W. L. Mao, Appl. Phys. Lett. **104**, 021917 (2014).
[11] J. Laverock, S. Kittiwatanakul, A. A. Zakharov, Y. R. Niu, B. Chen, S. A. Wolf, J. W. Lu, and K. E. Smith, Direct observation of decoupled structural and electronic transitions and an ambient pressure monocliniclike metallic phase of VO_2 (to be published).
[12] M. M. Qazilbash *et al.*, Science **318**, 1750 (2007).
[13] H.-T. Kim, B.-G. Chae, D.-H. Youn, S.-L. Maeng, G. Kim, K.-Y. Kang, and Y.-S. Lim, New J. Phys. **6**, 52 (2004).
[14] M. Hada, D. Zhang, A. Casandruc, R. J. Dwayne Miller, Y. Hontani, J. Matsuo, R. E. Marvel, and R. F. Haglund, Phys. Rev. B **86**, 134101 (2012).
[15] X. Yuan, W. Zhang, and P. Zhang, Phys. Rev. B **88**, 035119 (2013).
[16] V. R. Morrison, R. P. Chatelain, K. L. Tiwari, A. Hendaoui, A. Bruhacs, M. Chaker, and B. J. Siwick, Science **346**, 445 (2014).
[17] A. Cavalleri, Cs. Tóth, C. Siders, J. Squier, F. Ráksi, P. Forget, and J. Kieffer, Phys. Rev. Lett. **87**, 237401 (2001).
[18] M. Hada, K. Okimura, and J. Matsuo, Phys. Rev. B **82**, 153401 (2010).
[19] P. Baum, D.-S. Yang, and A. H. Zewail, Science **318**, 788 (2007).
[20] D. J. Hilton, R. Prasankumar, S. Fourmaux, A. Cavalleri, D. Brassard, M. El Khakani, J. Kieffer, A. Taylor, and R. Averitt, Phys. Rev. Lett. **99**, 226401 (2007).
[21] C. Kübler, H. Ehrke, R. Huber, R. Lopez, A. Halabica, R. Haglund, and A. Leitenstorfer, Phys. Rev. Lett. **99**, 116401 (2007).
[22] A. Pashkin, C. Kübler, H. Ehrke, R. Lopez, A. Halabica, R. F. Haglund, R. Huber, and A. Leitenstorfer, Phys. Rev. B **83**, 195120 (2011).
[23] S. Wall, D. Wegkamp, L. Foglia, K. Appavoo, J. Nag, R. F. Haglund, J. Stähler, and M. Wolf, Nat. Commun. **3**, 721 (2012).
[24] A. Cavalleri, T. Dekorsy, H. H. W. Chong, J. C. Kieffer, and R. W. Schoenlein, Phys. Rev. B **70**, 161102 (2004).
[25] M. van Veenendaal, Phys. Rev. B **87**, 235118 (2013).
[26] S. Wall, L. Foglia, D. Wegkamp, K. Appavoo, J. Nag, R. Haglund, J. Stähler, and M. Wolf, Phys. Rev. B **87**, 115126 (2013).
[27] H. Dachraoui, N. Müller, G. Obermeier, C. Oberer, S. Horn, and U. Heinzmann, J. Phys. Condens. Matter **23**, 435402 (2011).
[28] R. Yoshida *et al.*, Phys. Rev. B **89**, 205114 (2014).
[29] M. W. Haverkort *et al.*, Phys. Rev. Lett. **95**, 196404 (2005).
[30] N. B. Aetukuri *et al.*, Nat. Phys. **9**, 661 (2013).
[31] J. Nag, E. Andrew Payzant, K. L. More, and R. F. Haglund, Appl. Phys. Lett. **98**, 251916 (2011).
[32] See Supplemental Material at http://link.aps.org/supplemental/10.1103/PhysRevLett.113.216401 for additional details on experiments and calculations.
[33] T. C. Koethe *et al.*, Phys. Rev. Lett. **97**, 116402 (2006).
[34] Broadened by the independently determined experimental energy resolution (90 meV).
[35] M. K. Liu *et al.*, Phys. Rev. Lett. **111**, 096602 (2013).
[36] Note that the photoinduced structural dynamics at different fluences might dominate the optical response on different timescales.
[37] Photoinduced shifts of the chemical potential into the VB (CB) are excluded, as they would be reflected in the PE intensity at lower (higher) energies than the sample holder E_F, respectively.
[38] The fast dynamics on femtosecond time scales are overlapped with a lifetimeless two-photon photoemission signal of pump and probe pulses (through virtual states), which is accounted for in the fits by a delta function at time zero.
[39] G. Onida, L. Reining, and A. Rubio, Rev. Mod. Phys. **74**, 601 (2002).
[40] L. Hedin, Phys. Rev. **139**, A796 (1965).
[41] M. Gatti, F. Bruneval, V. Olevano, and L. Reining, Phys. Rev. Lett. **99**, 266402 (2007); M. Gatti, Ph.D. thesis, École Polytechnique, Palaiseau, France, 2007, http://etsf.polytechnique.fr/sites/default/files/users/matteo/matteo_thesis.pdf.
[42] R. Sakuma, T. Miyake,, and F. Aryasetiawan, Phys. Rev. B **78**, 075106 (2008).
[43] B. Lazarovits, K. Kim, K. Haule, and G. Kotliar, Phys. Rev. B **81**, 115117 (2010).
[44] A. Oschlies, R. W. Godby, and R. J. Needs, Phys. Rev. B **45**, 13741 (1992); **51**, 1527 (1995).
[45] R. Abram, G. Rees, and B. Wilson, Adv. Phys. **27**, 799 (1978).
[46] J. Wagner, Phys. Rev. B **32**, 1323 (1985).
[47] Y. Dou, T. Fishlock, R. G. Egdell, D. S. L. Law, and G. Beamson, Phys. Rev. B **55**, R13381 (1997).
[48] C. D. Spataru, L. X. Benedict, and S. G. Louie, Phys. Rev. B **69**, 205204 (2004).
[49] E. Dagotto, Science **309**, 257 (2005).
[50] M. Rini *et al.*, Appl. Phys. Lett. **92**, 181904 (2008).
[51] V. Eyert, Ann. Phys. (Berlin) **11**, 650 (2002).
[52] This is in agreement with Kim *et al.* [6,13]. However, in contrast to our work where we unambiguously prove the electronic origin of the PT, they use a weak laser to give the electronic PT a head start with respect to the structural PT when driving it thermally.